



Cite this: *Chem. Commun.*, 2016, 52, 1911

Received 18th November 2015,  
Accepted 4th December 2015

DOI: 10.1039/c5cc09536k

www.rsc.org/chemcomm

# An all-inorganic polyoxometalate–polyoxocation chemical garden†

Laurie J. Points,<sup>a</sup> Geoffrey J. T. Cooper,<sup>a</sup> Anne Dolbecq,<sup>b</sup> Pierre Mialane<sup>b</sup> and Leroy Cronin<sup>\*a</sup>

Herein, we show it is possible to produce wholly inorganic chemical gardens from a cationic polyoxometalate (POM) seed in an anionic POM solution, demonstrating a wholly POM-based chemical garden system that produces architectures over a wide concentration range. Six concentration dependent growth regimes have been discovered and characterized: clouds, membranes, slugs, tubes, jetting and budding.

Chemical gardens, also known as crystal or silicate gardens, are plant like structures which have fascinated scientists since they were first documented in the 17<sup>th</sup> century.<sup>1</sup> Classic chemical gardens form when a metal-salt ‘seed’ particle is added to an aqueous anion solution, often silicate, phosphate or carbonate, whilst polyoxometalate (POM) gardens grow from a POM seed and an organic or simple metal cation (Fig. 1A).<sup>2,3</sup> From this seed particle, hollow precipitation tubes grow, to resemble plants, giving chemical gardens their name. The field of chemical gardens has had a resurgence since the turn of the century and the field has recently been termed chemobrionics.<sup>2</sup> There are several variations on the classic chemical garden system. Reverse chemical gardens can be formed when a silicate seed is held at the top of a metal salt solution or when sodium silicate solution is injected into a metal salt solution.<sup>4–6</sup> Chemical gardens also share features with precipitation structures formed in Portland cement,<sup>7</sup> metal corrosion tubes,<sup>8</sup> brinicles and hydrothermal vents,<sup>9,10</sup> whilst a constrained 2D garden has been prepared within a Hele-Shaw cell.<sup>5,11</sup>

POMs are a diverse range of cluster compounds of molecular metal oxides, formed by oxo bridged early transition metals.<sup>12,13</sup> They may be considered as an intermediate between small molecules and infinite metal oxides as they exhibit many of the

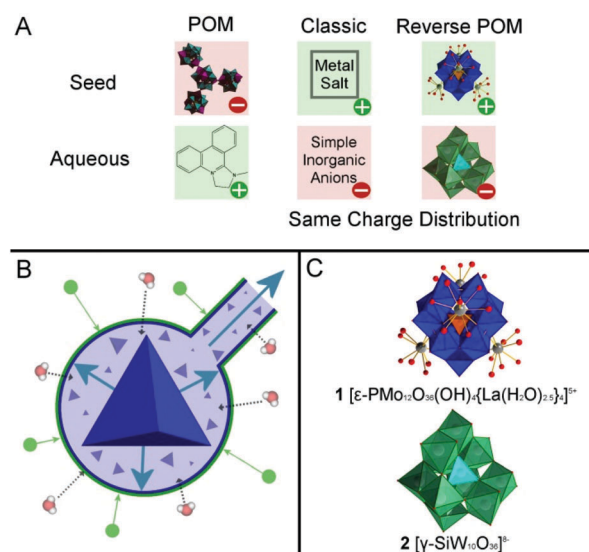


Fig. 1 (A) A graphical representation of some different types of chemical gardens that are known; previously reported POM chemical gardens, classic chemical gardens and the charge reversed POM chemical gardens presented herein. (B) A schematic representation of the general POM chemical garden growth mechanism. (C) Structures of the POMs used in this study. Blue – Mo, Orange – P, Grey – La, Red – O, Green – W, Teal – Si.

properties of bulk metal oxides in a discrete molecular entity. POMs can form a diverse range of structures which in turn have a great number of properties and potential applications.<sup>14,15</sup> Previously we were able to show that the anionic character of the large POM clusters could be used to form chemical gardens when placed in aqueous organic cation solutions,<sup>16</sup> but this phenomenon was limited to organic cations and transition metal complexes.<sup>17</sup> Given it is possible to externally control the architecture of the hybrid organic–inorganic tubes,<sup>18</sup> we wondered if this could be extended to all inorganic systems.

Herein, we describe how we were able to achieve the goal of realizing an all-inorganic metal oxide chemical garden system. We did this by utilizing a POM system consisting of

<sup>a</sup> WestCHEM, School of Chemistry, University of Glasgow, University Avenue, Glasgow, G12 8QQ, UK. E-mail: lee.cronin@glasgow.ac.uk

<sup>b</sup> Institut Lavoisier de Versailles, UMR 8180, Université de Versailles Saint-Quentin en Yvelines, Université Paris Saclay, 45 Avenue des Etats-Unis, 78035 Versailles cedex, France

† Electronic supplementary information (ESI) available: Additional images, videos and full experimental details. See DOI: 10.1039/c5cc09536k



$[\epsilon\text{-PMo}_{12}\text{O}_{36}(\text{OH})_4\{\text{La}(\text{H}_2\text{O})_{2.5}\}_4]^{5+}$  **1** and  $[\gamma\text{-SiW}_{10}\text{O}_{36}]^{8-}$  **2**, which overcomes the differences between POM based and classic chemical garden systems, both in terms of their charge distribution and the presence of aqueous organic or transition metal cations. Whilst POM based chemical garden growth has been shown for anionic POM seeds within a certain solubility range,<sup>17</sup> charge inversion represents a significant generalization of this phenomena. Furthermore, classic chemical gardens require high anion concentrations, whereas in this work precipitation structures are observed at concentrations as low as 0.5 mM, orders of magnitude below its solubility limit.

To prepare a POM based chemical garden with a cationic seed crystal, such a positively charged POM needed to be identified, and these are incredibly rare. However  $[\epsilon\text{-PMo}_{12}\text{O}_{36}(\text{OH})_4\{\text{La}(\text{H}_2\text{O})_{2.5}\text{Cl}_{1.25}\}_4]$  **1**, reported by Mialane *et al.* in 2002, is a good candidate.<sup>19</sup> These polyoxocations have the rare  $\epsilon$ -Keggin structure, with a central phosphorous atom and four capping  $\{\text{La}(\text{H}_2\text{O})_4\}^{3+}$  groups stabilizing the structure and giving it its net positive charge (Fig. 1C). For the anionic constituent, potassium  $\gamma$ -decaturstosilicate ( $\text{K}_8[\gamma\text{-SiW}_{10}\text{O}_{36}]$ ) **2** was used due to the ease of its synthesis and its measured solubility in water at room temperature of  $150.4 \text{ mg mL}^{-1}$ . This is well above the  $5 \text{ mg mL}^{-1}$  minimum solubility limit for the aqueous component in POM based chemical gardens previously reported,<sup>17</sup> although this limiting value is likely to be significantly different for these charge-inverted systems. When a solution of **2** (1–20 mM) was added to crystals of **1**, tubes were seen to grow out of the seed crystal, see Fig. 2. At concentrations at the higher end of this spectrum tube growth was rapid, whereas at lower concentrations tube growth was slower, with a noticeable initiation time present at the lowest concentrations. As such, this system is suitable for investigating reverse POM based chemical garden systems.

The tube growth mechanism can be explained with reference to Fig. 1B. Initially, when the POM crystal is placed in the anion solution, a semi-permeable membrane forms around the crystal

as it dissolves. As the bulky cations come into contact with bulky POM anions, ion exchange occurs causing precipitation to form a membrane. As neither POM species can cross this semi-permeable membrane, an osmotic pump initiates. The pressure then increases to the point that the membrane ruptures, and it is from this aperture that tube growth initiates. As water continues to flow into the membrane, this continues to push polyoxocation out of the growing tube, where it will meet POM and precipitate, forming the tube wall.

Having identified a suitable system for charge-inverted tube growth, experiments were undertaken with **2** present in the aqueous phase at concentrations of 0.5–30.0 mM to investigate the effect of concentration on the precipitation structures formed (see ESI videos SV1–6†). At low concentrations ( $<1 \text{ mM}$ , Fig. 3, left), precipitation clouds form. At higher concentrations the precipitation occurs quickly enough to form a membrane, followed by a period of dormancy as the pressure increases. When the membrane bursts a tube will grow from the burst point. This doesn't always occur, but if it does only one tube is formed and it is typically short, with a relatively small area. This is because a significant amount of material is required to form the membrane coupled with the low solution concentration giving wide tubes. The membranes are resilient enough to withstand SEM analysis, which confirmed that they are 3-dimensional in nature (see ESI†).

As the concentration rises from 2–20 mM the tubes formed have increasing aspect ratios and cover a smaller area. The tubes form under a set of six different growth regimes, here called (i) clouds, (ii) membranes, (iii) slugs, (iv) tubes, (v) jetting and (vi) budding. Another point to note is the precipitate clouds present around the growing tube heads (see ESI videos SV2–5 and Fig. S5 and S6†), which are especially prominent at lower concentrations, reminiscent of the umbrella like plume heads in classic chemical gardens.<sup>20</sup> At anion concentrations of 30 mM or above no membrane formation or tube growth occurs.

Classic chemical gardens involve precipitation structures growing vertically from the seed crystal due to the lower density of the metallic solution compared to the silicate solution. In charge-normal POM based systems, however, tube growth is primarily two-dimensional, with tubes growing on the glass slide due to the higher density of POM solution compared to the surrounding cation solution. In this system the picture is slightly more complicated. Larger, slug-like tubes grow on the surface of the glass slide but the faster growing smaller tubes often grow away from the surface, as their momentum is enough to overcome their negative buoyancy and they grow in whatever direction they face as the membrane ruptures. Previous POM based chemical garden systems have also been shown to continue growing until all of the seed material is used up, leaving a crystal shell at the base of the tube.<sup>17</sup> This is not the case for the system presented here, in which tube growth terminates whilst material remains present in the seed crystal. Another interesting feature of this system is that microcrystallites can be seen to grow in tubes, as can be seen in SV7 and Fig. S6 and S32,† which also often initiate mass precipitation within the tube. Tube growth can be completed over a shorter

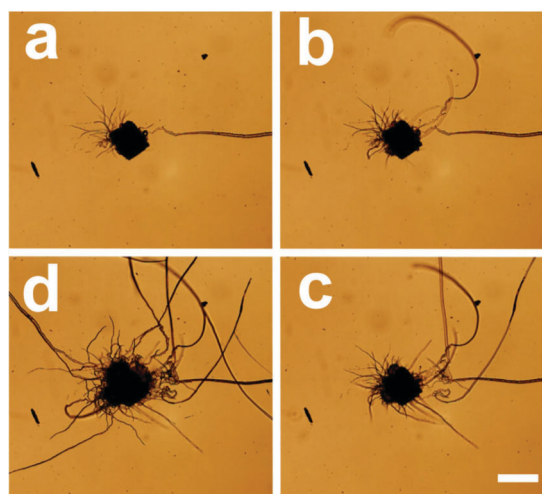


Fig. 2 Photos from SV6† showing tube growth at 20 mM after 10 (a), 40 (b), 70 (c) and 220 (d) seconds. Scale bar is  $200 \mu\text{m}$ .



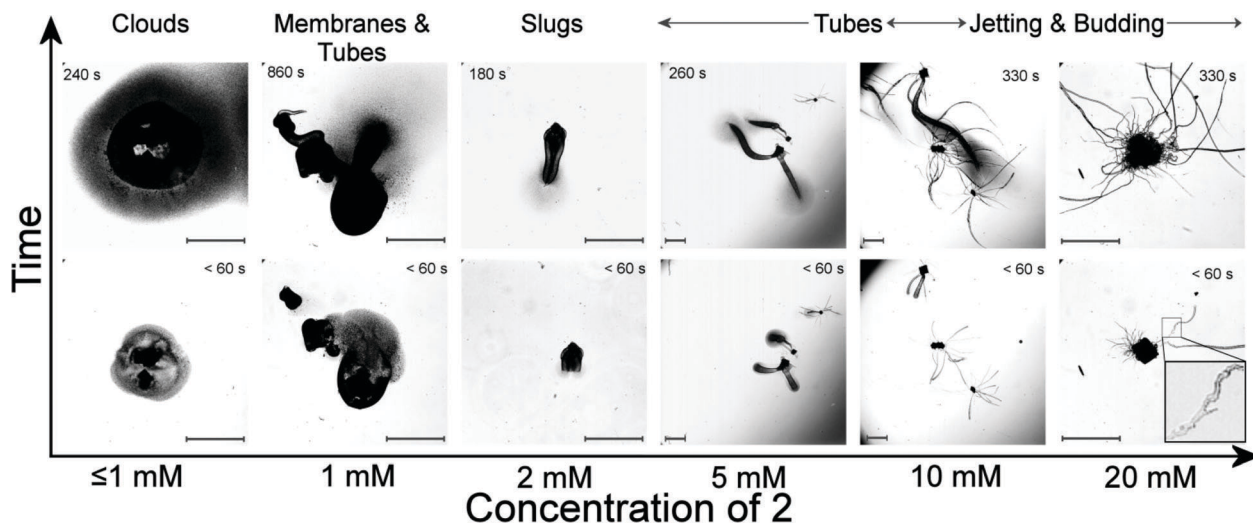


Fig. 3 The range of precipitation structures observed for the polyoxometalate–polyoxocation system described here, ranging from cloud like structures at low concentrations to jetting and budding tubes at higher concentrations. Inset on lower 20 mM figure highlights the budding growth regime. Scale bars = 400  $\mu\text{m}$ .

timescale at all concentrations for this reverse system compared to charge-normal systems (20 min vs. hours).

In the synthesis of **1**, a large excess of  $\text{LaCl}_3$  is used to help push the equilibrium toward the complex with four capping  $[\text{La}(\text{H}_2\text{O})_4]^{3+}$  groups, giving the overall 5+ charge. In the tube growing system, the only lanthanum present is that in the crystal. It has been shown by NMR spectroscopy that in pure water the  $[\epsilon\text{-PMo}_{12}\text{O}_{36}(\text{OH})_4\{\text{La}(\text{H}_2\text{O})_{2.5}\}_4]^{5+}$  affords the  $[\epsilon\text{-PMo}_{12}\text{O}_{36}(\text{OH})_4\{\text{La}(\text{H}_2\text{O})_{2.5}\}_3]^{2+}$  POM. Moreover, it has also been evidenced by X-ray diffraction that this dicationic species evolves to the  $[\epsilon\text{-PMo}_{12}\text{O}_{36}(\text{OH})_4]^{5-}$  lanthanum-free anion.<sup>19</sup> In the tube growth system, flame atomic absorption/emission spectroscopies have shown that the La : Mo ratio is significantly higher than expected in the supernatant solution, indicating a higher level of incorporation of lanthanum into the precipitation structures. As the complex becomes anionic by subsequent  $\text{La}^{3+}$  loss, it will no longer precipitate with the anionic **2**, preventing tube growth.

Despite the fact that tube growth does not continue until the crystalline material is consumed, there is a linear correlation between the crystal and tube surface areas, as shown in Fig. 4. This trend is strong considering such factors as crystal volume not necessarily correlating to measured surface area; the fact that some crystals are in fact several crystals merged together and natural variation in factors such as tube growth speed and termination point. In this all inorganic crystal garden POM-system, the tube growth rates was found to show an exponential trend, without normalizing for the crystal surface area, as shown in Fig. 5. This is significantly different to previous findings for POM based chemical gardens where growth rate, when normalized to the crystal surface area, was found to be linearly proportional to the cation concentration.<sup>9,10</sup> The reason for this is unclear, although it is worth noting the significantly larger concentration range presented for this system (for the previously reported system, the concentration range was 0.5–3.5 mM).

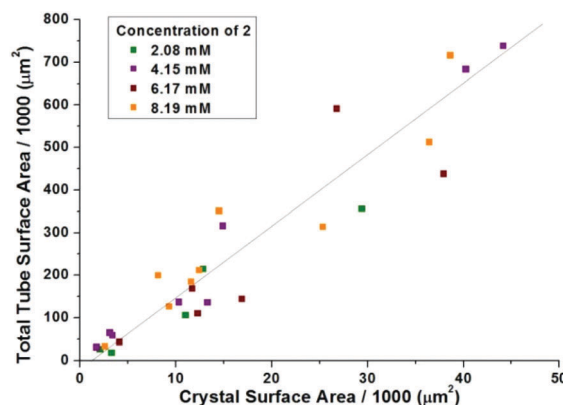


Fig. 4 A plot showing the linear correlation between the crystal surface area and the tube surface area formed, when measured from above. Guideline to illustrate trend only.

Unlike for charge-normal POM chemical gardens, both gradual and step changes in the tube diameter are observed, as illustrated in Fig. 3 and S7.† These are most likely to be due to initiation, termination and merging events in other tubes growing from the same crystal. In the charge-normal systems one tube is typically observed, hence these events could not occur, although these observations could also point to mechanistic differences in this system (Fig. 5). Diameter changes can also be induced by changing the anion concentration during tube growth, as shown in Fig. S7.†

In conclusion, we have demonstrated a wholly inorganic polyoxometalate based chemical garden system by using a polyoxocationic seed crystal in a dilute aqueous polyoxometalate solution. This work bridges a significant gap between POM based chemical gardens and classic chemical gardens as it has the same charge distribution as classic chemical gardens. Qualitative variations in tube morphology at differing anion



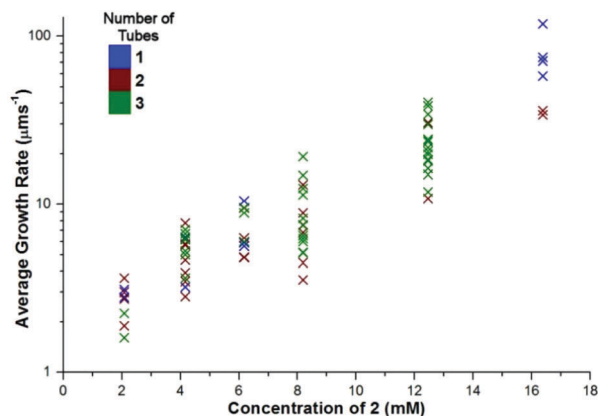


Fig. 5 A plot showing the exponential trend between the anion (2) concentration and the tube growth rate.

concentrations have been described, and six growth regimes observed, here termed clouds, membranes, slugs, tubes, jetting and budding. As the anion concentration is raised, each of these growth regimes is observed, with an associated increasing aspect ratio and number of tubes. Quantitative data has been obtained from optical microscopy which has demonstrated that the tube surface area deposited from a crystal is linearly related to the crystal surface area. This is despite the fact that, unlike previously reported systems, tube growth terminates before all the parent seed material is consumed. An exponential trend has also been observed between the anion concentration and the tube growth rate. In future, the development of a numerical model for this rather complex system would represent a significant contribution to this growing field. POM based chemical gardens provide another system that may be used to understand the general chemical garden growth phenomenon, whilst there is also potential for them to be applied in fields such as catalysis and advanced materials, taking advantage of the inherent properties of their polyoxometalate constituents.

We thank the EPSRC grants (No. EP/J015156/1; EP/L023652/1; EP/I033459/1; EP/J015156/1; EP/K023004/1; EP/L023652/1), EC grant

318671 MICREAGENTS. LC thanks the Royal Society/Wolfson Foundation for a Merit Award. We also thank Mr James Gallagher (SEM) and Mr Michael Beglan (Elemental Analysis).

## Notes and references

- 1 J. R. Glauber, in *Furni Novi Philosophici*, English translation, ed. C. Packe, London, 1689; Amsterdam, 1646.
- 2 L. M. Barge, S. S. S. Cardoso, J. H. E. Cartwright, G. J. T. Cooper, L. Cronin, A. De Wit, I. J. Doloboff, B. Escibano, R. E. Goldstein, F. Haudin, D. E. H. Jones, A. L. Mackay, J. Maselko, J. J. Pagano, J. Pantaleone, M. J. Russell, C. I. Sainz-Díaz, O. Steinbock, D. A. Stone, Y. Tanimoto and N. L. Thomas, *Chem. Rev.*, 2015, **115**, 8852.
- 3 R. Makki, L. Roszol, J. J. Pagano and O. Steinbock, *Philos. Trans. R. Soc. London, Ser. A*, 2012, **370**, 2848–2865.
- 4 S. Thouvenel-Romans and O. J. Steinbock, *J. Am. Chem. Soc.*, 2003, **125**(14), 4338.
- 5 J. J. Pagano, T. Bansagi and O. Steinbock, *J. Phys. Chem. C*, 2007, **111**(26), 9324.
- 6 F. Haudin, J. H. E. Cartwright and A. De Wit, *J. Phys. Chem. C*, 2015, **119**, 15067–15076.
- 7 D. D. Double and A. Hellawell, *Nature*, 1976, **255**, 486.
- 8 D. A. Stone and R. E. Goldstein, *Proc. Natl. Acad. Sci. U. S. A.*, 2004, **101**(32), 11537.
- 9 J. H. E. Cartwright, B. Escibano, D. L. González, C. I. Sainz-Díaz and I. Tuval, *Langmuir*, 2013, **29**, 7655.
- 10 M. J. Russell and A. J. Hall, *J. Geol. Soc.*, 1997, **154**(3), 377.
- 11 F. Haudin, J. H. E. Cartwright, F. Brau and A. De Wit, *Proc. Natl. Acad. Sci. U. S. A.*, 2014, **111**(49), 17363.
- 12 D.-L. Long, R. Tsunashima and L. Cronin, *Angew. Chem., Int. Ed.*, 2010, **49**, 1736–1758.
- 13 P. Gouzerh and M. Che, *Actual. Chim.*, 2006, **298**, 9–22.
- 14 Q. Yin, J. M. Tan, C. Besson, Y. V. Geletii, D. G. Musaev, A. E. Kuznetsov, Z. Luo, K. I. Hardcastle and C. L. Hill, *Science*, 2010, **328**, 342–345.
- 15 J. T. Rhule, C. L. Hill, D. A. Judd and R. F. Schinazi, *Chem. Rev.*, 1998, **98**, 327–357.
- 16 C. Ritchie, G. J. T. Cooper, Y.-F. Song, C. Streb, H. Yin, A. D. C. Parenty, D. A. MacLaren and L. Cronin, *Nat. Chem.*, 2009, **1**, 47.
- 17 G. J. T. Cooper, A. G. Boulay, P. J. Kitson, C. Ritchie, C. J. Richmond, J. Thiel, D. Gabb, R. Eadie, D.-L. Long and L. Cronin, *J. Am. Chem. Soc.*, 2011, **133**(15), 5947.
- 18 G. J. T. Cooper, R. W. Bowman, E. P. Magennis, F. Fernandez-Trillo, C. Alexander, M. J. Padgett and L. Cronin, *Angew. Chem., Int. Ed.*, 2012, **51**, 12754.
- 19 P. Mialane, A. Dolbecq, L. Lisnard, A. Mallard, J. Marrot and F. Sécheresse, *Angew. Chem., Int. Ed.*, 2002, **41**(13), 2398.
- 20 B. C. Batista, P. Cruz and O. Steinbock, *Langmuir*, 2014, **30**, 9123.

